Affiliates Program Meeting 2023

November 8th, 2023

Hybrid RANS Modeling of Jet Noise

Tejal Shanbhag, Gao Jun Wu, Beckett Zhou, Sanjiva Lele, Juan Alonso

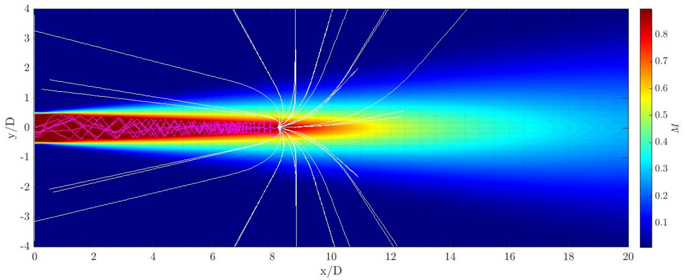

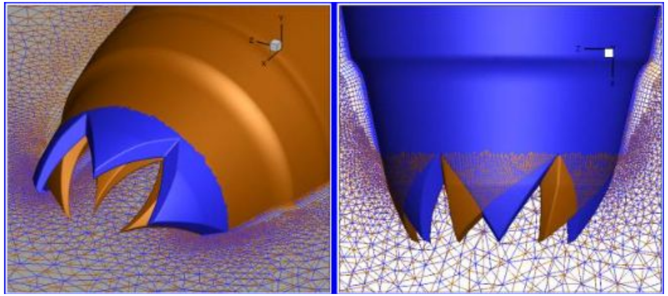

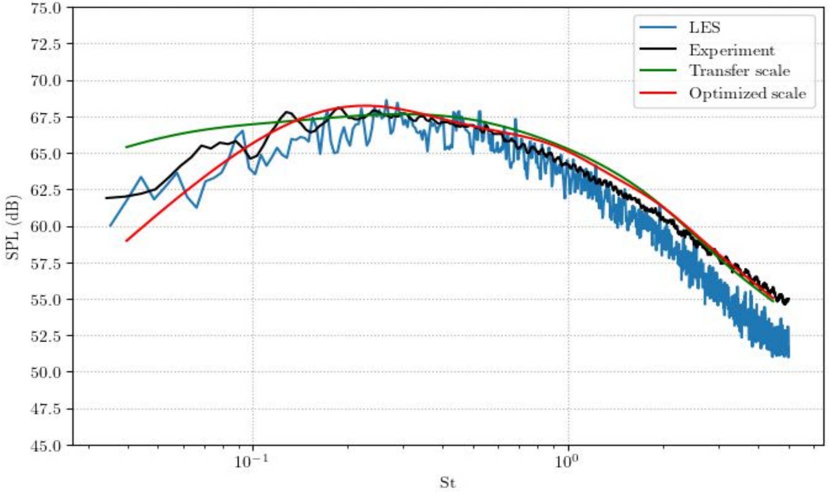

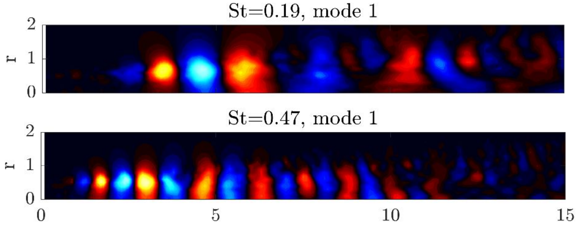

Multifunctional Energy Storage Composites for the Next Generation of Electric Vehicles

Professor Fu-Kuo Chang || Presenter: Giavanna Angelo

Main Transportation of the Future

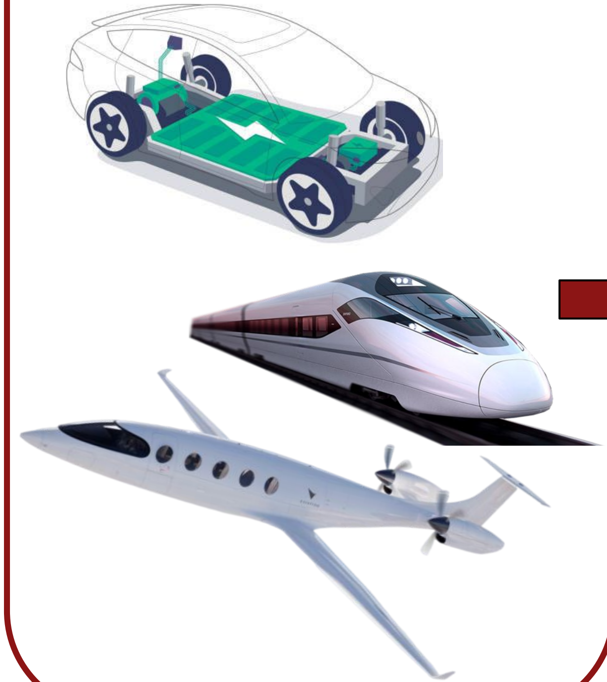

Limitations

High combustibility leads to:

- **Increased weight** caused by extra protection structures for safety
- **Conservative design** required for battery health management system

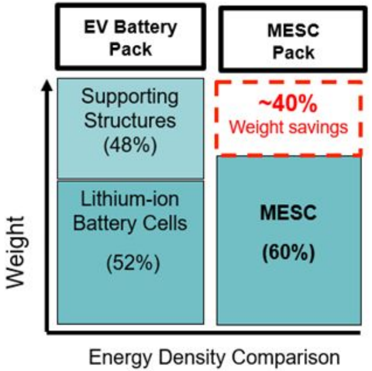

MESC

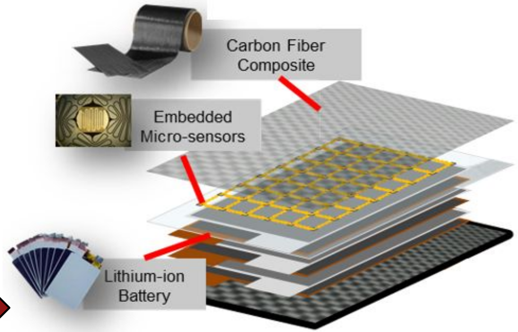

MESC integrates:

- Battery Material
- Composite Structure
- Health Monitoring

together into **one multifunctional** system

Closed-form Optimal Propulsive-Differential Drag Control of Spacecraft Swarms

Matthew Hunter, Simone D’Amico

Stanford Space Rendezvous Laboratory
slab.stanford.edu

- **Hybrid control**: accomplish large reconfigurations with limited propellant by incorporating differential drag
- **Reachable set theory**: geometrically identifies analytical minimum costs and optimal maneuver times
- Closed-form solver matches **optimal cost** and final state error of numerical solvers while running in **linear time**

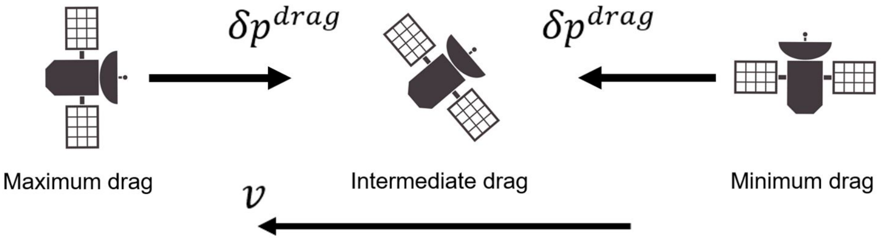

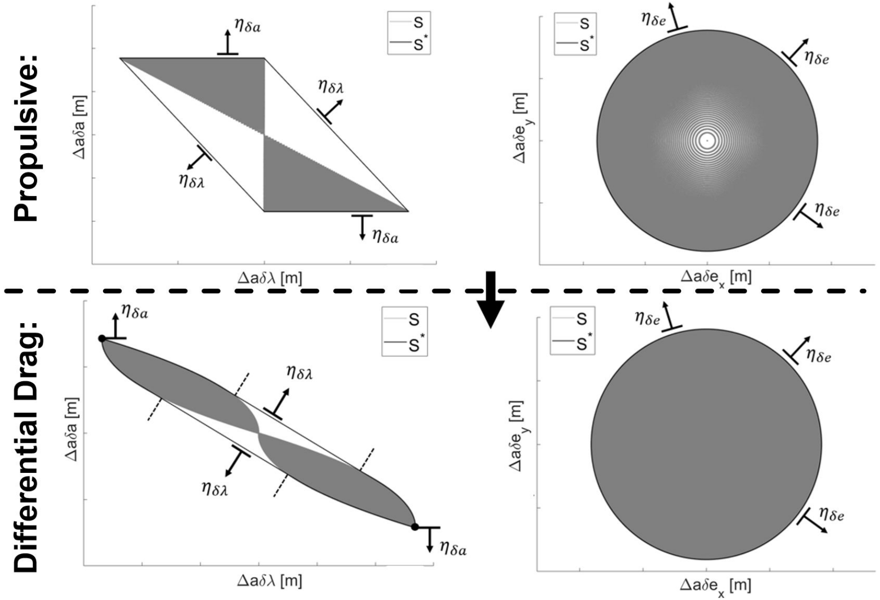

Exoplanet Detection from Starshade Images Using Convolutional Neural Networks

Zahra Ahmed, Simone D’Amico, Renyu Hu, Mario Damiano

Stanford Space Rendezvous Laboratory
slab.stanford.edu

- High-contrast, direct imaging is necessary for the discovery and characterization of **habitable worlds**
- **Starshades** are a promising starlight suppression technology
- There is a need for **post-processing algorithms** that can efficiently process large volumes of data

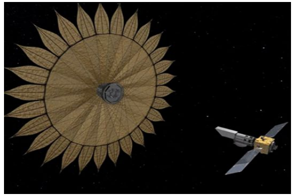

Credit: NASA/JPL

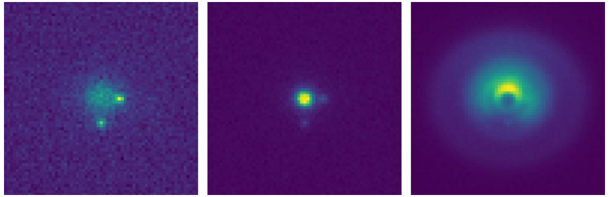

New Approach: Convolutional Neural Networks

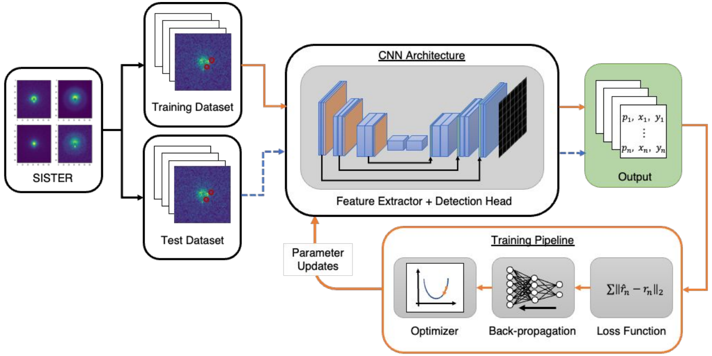

An Innovative Approach to Detecting Sub-centimeter Orbital Debris in Space

SESS
Space Environment and Satellite Systems
STANFORD
UNIVERSITY

Ashwyn Sam, PhD Candidate, Prof. Sigrid Elschot
(Space Environment and Satellite Systems (SESS) Lab)

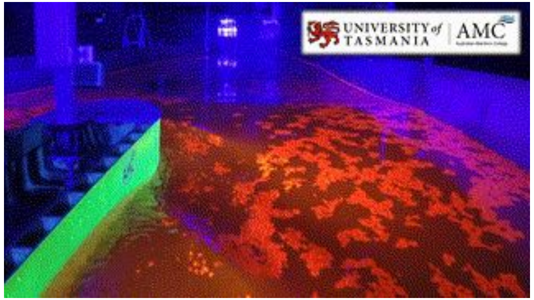

Soliton water waves moving ahead of and faster than ship

- Charged objects traversing through plasma can generate solitons that move ahead of the debris
- Can we use these solitons to detect the debris before collision?
- In theory, yes! Simulations show that the amplitude of these waves should be detectable by existing sensor technology

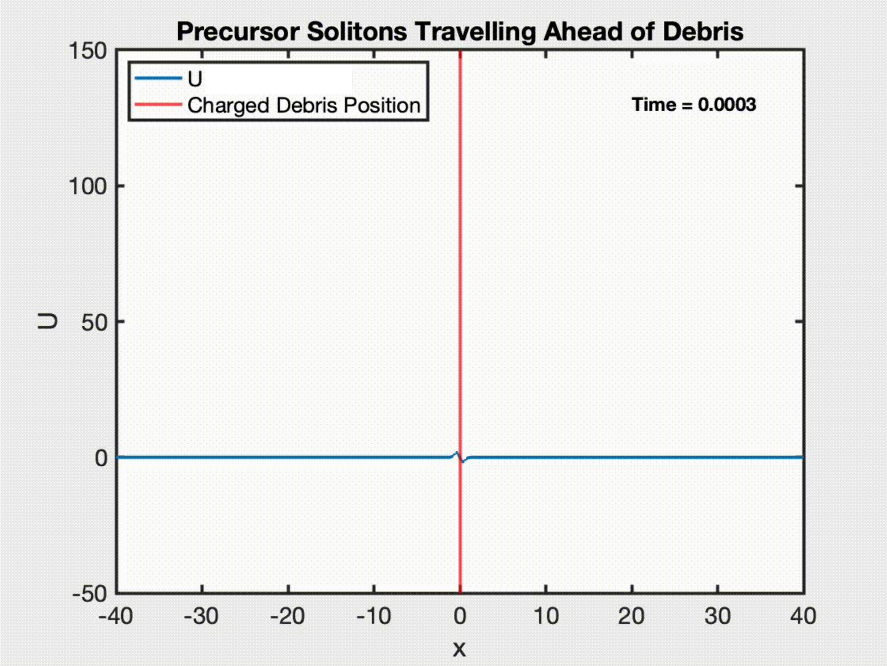

Stanford
University

Advancing the state-of-the-art in the simulation of supersonic parachute inflation dynamics

Faisal As'ad, Philip Avery, Charbel Farhat

What is the problem?

Supersonic parachute inflation dynamics (PID) is a highly complex physical phenomenon governed by intricate flow features interacting with a porous heterogeneous canopy membrane and thin suspension lines. A concrete theoretical understanding of these phenomena remains unavailable. Consequently, the development of a **computational framework** to simulate SPID numerically is imperative to obtaining an understanding of the underlying physical mechanisms and sensitivities. However, this forms a formidable challenge, from both modeling and computational perspectives. Farhat Research Group has been working on this problem for several years now through the development of the **AERO Suite** multi-physics computational framework[1, 2]: our goal is to pursue advancing the state-of-the-art of PID.

Why does it matter?

NASA uses parachutes in the supersonic regime to land their rovers on Mars. However, each generation of rovers is getting heavier and heavier. This means that the parachutes are subjected to larger loads and thus more susceptible to **failure**. In fact, the largest supersonic parachute deployed by NASA, with a diameter of 30 m, failed in back-to-back flight tests in 2014 and 2015 at loads significantly lower than their design load.

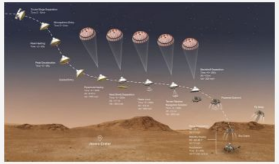

Flight tests are expensive and do not offer much insight...this is where numerical simulations can shine!

Simulation of the ASPIRE SR03 flight test

The ASPIRE SR03 flight test served as a qualification test for the Disk-Gap-Band parachute system of the Perseverance rover that landed on Mars in February 2021.

We aim to validate AERO Suite for capturing the two-way interaction of the supersonic fluid and the parachute system by accurately reproducing the flight test results with our simulations.

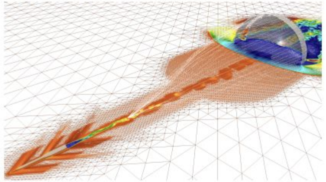

We validate the simulation results gainst drag data measured from flight test, and we obtain good agreement

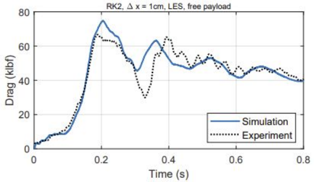

Identifying the areas of maximum stress from these simulations can be crucial for predicting and mitigating parachute failure.

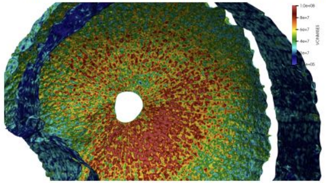

Multiscale modelling of canopy fabric

The parachute canopy is a very heterogeneous structure.

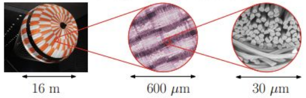

The buckling of the fibers and the friction between them give rise to nonlinear and time-dependent behavior at the macro-scale.
Due to the disparity between the scales, a FE simulation that resolves all scales is computationally intractable. Therefore, we have developed a `FEM`^{2} homogenization scheme compatible with plane-stress elements within AERO Suite.

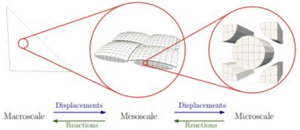

Because the FE-based homogenization scheme is computationally intensive, we use it only to generate training data for a **mechanics-informed viscoelastic ANN-based constitutive law**[3, 4]. The ANN framework is expressed in terms of three convex ANNs (W, V, G) and satisfies, by construction, important mechanical constraints:

- dynamic/static stability
- consistency
- objectivity
- limiting behaviors
- 2nd law of thermodynamics

$$\boldsymbol{S} = \frac{\partial W}{\partial \boldsymbol{E}}(\boldsymbol{E}) + \frac{\partial V}{\partial \boldsymbol{E}}(\boldsymbol{E}, \boldsymbol{\alpha})$$
$$\dot{\boldsymbol{\alpha}} = \frac{\partial G}{\partial \boldsymbol{\beta}}(\boldsymbol{\beta}, \boldsymbol{E})$$
$$\boldsymbol{\beta} = -\frac{\partial V}{\partial \boldsymbol{\alpha}}(\boldsymbol{E}, \boldsymbol{\alpha})$$

The resulting constitutive law is robust to noise and can extrapolate accurately to unseen inputs. It is also stable and physically meaningful when used in FE simulations.

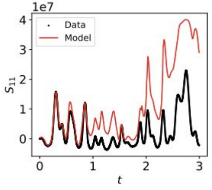

Vanilla ANN

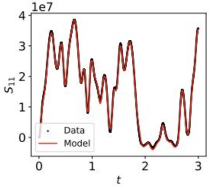

Mechanics-informed ANN

Multiscale modeling of braided suspension lines

We also take a multiscale approach to modeling the braided suspension lines.

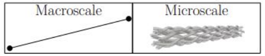

We fit the `FEM`^{2} homogenized data fitted by a heuristic parametric model.

$$S_{11} = A\left[\ln\left(\left(e^{C} - 1\right)e^{BE_{11}} + 1\right) - C\right]$$

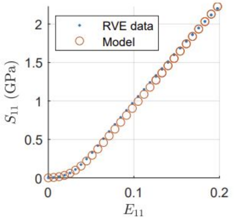

References

[1] Daniel Z Huang, Philip Avery, Charbel Farhat, Jason Rabinovitch, Armen Derkevorkian, and Lee D Peterson. Modeling, simulation and validation of supersonic parachute inflation dynamics during mars landing. In *AIAA Scitech 2020 Forum*, page 0313, 2020.

[2] Faisal As'ad, Philip Avery, Charbel Farhat, Jason Rabinovitch, and Marcus Lobbia. Validation of a high-fidelity supersonic parachute inflation dynamics model and best practice. In *AIAA SCITECH 2022 Forum*, page 0351, 2022.

[3] Faisal As'ad and Charbel Farhat. A mechanics-informed deep learning framework for data-driven nonlinear viscoelasticity. *Computer Methods in Applied Mechanics and Engineering*, 417:116463, 2023.

[4] Faisal As'ad, Philip Avery, and Charbel Farhat. A mechanics-informed artificial neural network approach in data-driven constitutive modeling. *International Journal for Numerical Methods in Engineering*, 123(12):2738–2759, 2022.

Graph Neural Networks for Improving GPS Positioning

Adyasha Mohanty and Grace Gao

- Urban GPS positioning challenging due to blocked and reflected signals
- Hybrid approaches promising for improving positioning accuracy

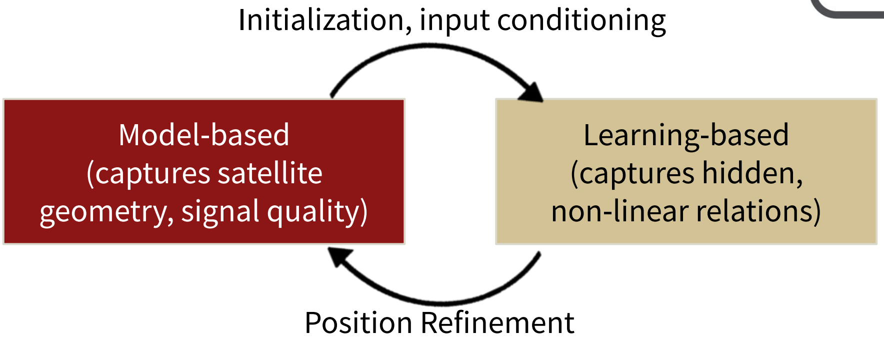

Initialization, input conditioning

Model-based (captures satellite geometry, signal quality)

Learning-based (captures hidden, non-linear relations)

Position Refinement

- **Our approach** deeply couples a **learned Kalman filter** with a **Graph Neural Network (GNN)** by jointly updating both in a **unified framework**

GNN uses Kalman filter-conditioned features, cosine-similarity based edges and adapts to dynamic graphs

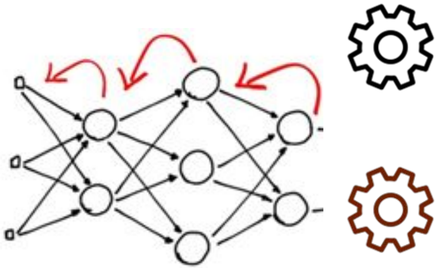

Adaptive Kalman filter parameters updated by making the filter differentiable and using backpropagation

Three-Dimensional Effects of Kinetic Instabilities in Hall Effect Thrusters

Andrew Denig (PhD Candidate), Ken Hara (Advisor)

- Hall Effect Thruster Operation: Neutral gas injected → ionized by electrons in chamber.
- Confinement time of electrons crucial for thruster performance (e.g., thrust, efficiency).
- **Plasma turbulence** is one of the main potential causes of *anomalous* electron transport.
  - Characterizing and modeling the instabilities that initiate such turbulence is necessary to quantify electron transport.
- Wave behavior in 3D [3] is different than 1D or 2D…additional kinetic effects!
  - Damping of waves due to wave-particle interactions.
  - Thermal motion along magnetic field lines.
  - Plasma sheath dynamics coupling to waves [4].

Hall effect thruster [1]

Front view

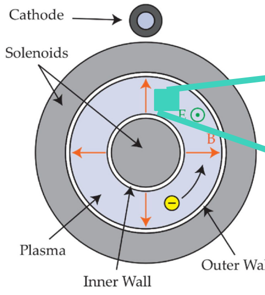

Side view

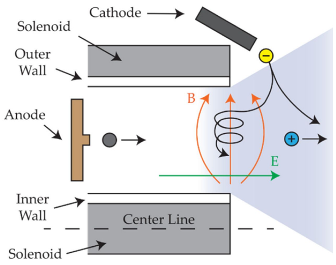

2D PIC Simulation Domain [2]:

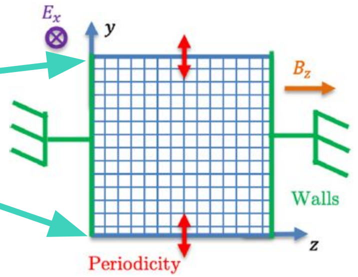

y: (**k** ⊥ **B**)

z: (**k** // **B**

[1] Lafleur, Baalrud, and Chabert, *Phys. Plasmas* **23**, 053503 (2016).
[2] Villafana, Petronio, Denig, … Hara, … et al., *Plasma Sources Sci. Technol.* **30**, 075002 (2021).
[3] Denig and Hara, Phys. Plasmas **30** 032108 (2023).
[4] Denig and Hara, IEPC-2022-345, Cambridge, MA, June 2022.

PDML

Stanford University

Using **POMDPs** to inform mining actions to aid the U.S. in developing a **lithium supply chain**

By: Yasmine Alonso, B.S. CS 2025, Prof. Mykel Kochenderfer

U.S. desires **self-sufficiency** in its lithium supply

But, we do not have the necessary infrastructure → must collaborate with friendly countries (i.e., Australia)

Lithium deposits are **highly uncertain**

Determine an **optimal sequence** of mine/explore actions to **maximize volume mined** and **minimize carbon emissions**

GitHub Repo

SISL
Stanford Intelligent Systems Laboratory

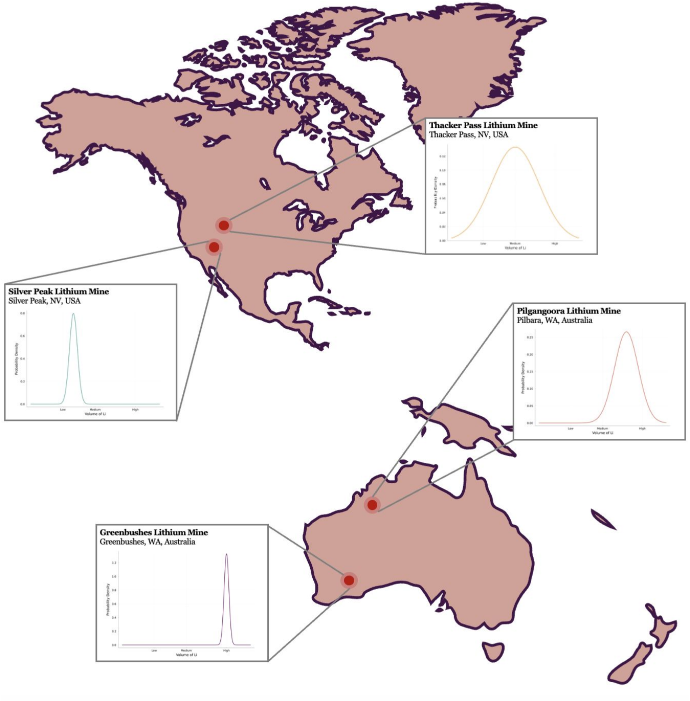

Current model with 4 potential lithium deposits.

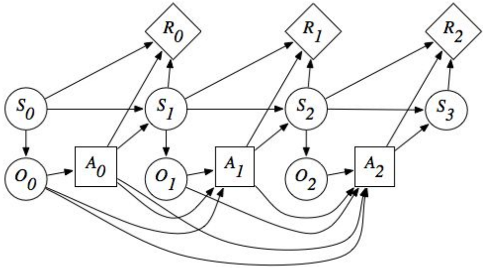

A partially observable Markov decision process (POMDP).

Table 1: A variety of policies/planners and their rewards.

Policy	Total Reward	Disc. Reward
RandomPolicy	14.95 ± 3.53	11.16 ± 2.07
EfficiencyPolicy	30.24 ± 0.11	23.79 ± 0.13
EmissionAwarePolicy	32.52 ± 0.15	25.83 ± 0.16
POMCPOW	22.87 ± 3.69	17.69 ± 2.89
MCTS-DPW	31.78 ± 1.90	25.37 ± 1.57

Table 2: A variety of policies/planners and their CO_2 emissions.

Policy	Total CO_2	Disc. CO_2
RandomPolicy	41.70 ± 2.34	36.12 ± 2.07
EfficiencyPolicy	62.4 ± 0.60	56.34 ± 0.68
EmissionAwarePolicy	55.50 ± 0.50	50.18 ± 0.58
POMCPOW	43.65 ± 1.67	37.99 ± 1.85
MCTS-DPW	36.05 ± 2.54	31.69 ± 2.24

Presenter:
Hang Song
PhD Candidate

Advisor:
Prof. Sanjiva K. Lele

Keywords:
Large-Eddy Simulations (LES), High-Order Numerics, Compressible Turbulence, High-Speed Aerodynamics, Shock Waves, High-Performance Computing (HPC), Real-Gas Effects (Transcritical Flows)

High-Resolution Simulations of Compressible Turbulent Flows

Hang Song[1, 2], Aditya S. Ghate[1, 3], Kristen V. Matsuno[1, 3], Jacob R. West[1, 2], Akshay Subramaniam[1, 3], Man-Long Wong[1, 3], Anjini Chandra[1, 2], Steven Dai[1, 2], Sanjiva K. Lele[1, 2, 3]
Flow Physics and Aeroacoustics Laboratory[1], Department of Mechanical Engineering[2], Department of Aeronautics & Astronautics[3], Stanford University

Motivation

This work develops a robust computational framework for simulations of compressible turbulent flows using high-order compact finite difference methods. Additionally, a massively scalable parallel algorithm is designed for large-scale simulations.

The project is primarily motivated by
- Growing interest from industry in LES
- Demands of large-scale DNS and LES in aerospace research
- Efficient use of leadership high-performance computing resources

High-resolution numerical framework

- Sixth-order compact finite-difference methods
- Fully-collocated variable storage and staggered flux assembly
  - ✓ Intrinsic aliasing error reduction
  - ✓ Improved accuracy of viscous operator at small scales
- Localized shock capturing schemes
- Geometric conservation law (GCL) consistent metric evaluation on curvilinear meshes
- Directly solves compressible Navier-Stokes equations in conservation form with robustness. No solution filtering is required.

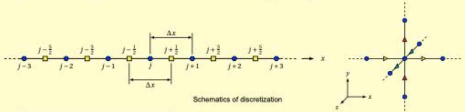

Schematics of discretization

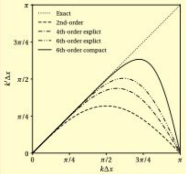

Modified wavenumber profiles of several collocated central difference schemes

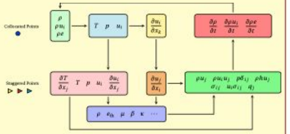

Schematic of time advancement process

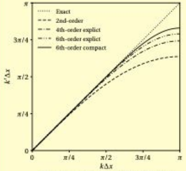

Modified wavenumber profiles of several staggered central difference schemes

Ongoing developments:
- Multi-component flow solver
- Multi-phase flow solver
- Application to aeroacoustics
- Adaptive mesh resolution

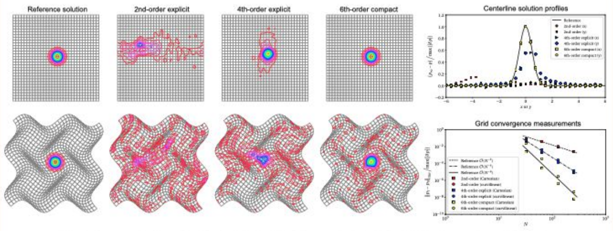

Advection of homentropic swirl on a 2D periodic domain simulated using different numerical methods. The simulations do not contain numerical dissipation.

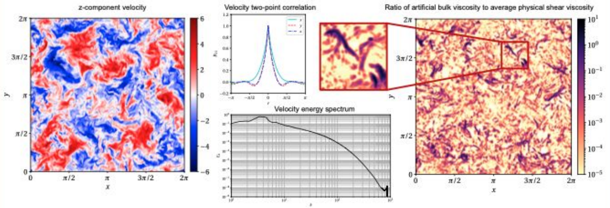

Direct numerical simulation of stochastically forced compressible isotropic turbulence at $M_t \approx 0.7$ and $Re_\lambda \approx 170$. Localized artificial bulk viscosity and conductivity are used to capture eddy shocklets. The solution filtering, claimed to be necessary in similar simulations, is no longer required.

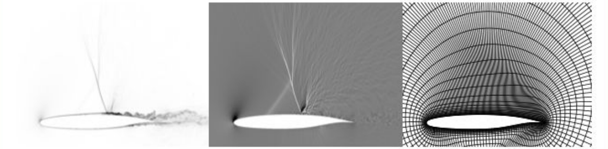

Numerical Schlieren imaging

Velocity dilatation

Downsampled computational mesh

Large-eddy simulation of transonic flow over OALT25 supercritical airfoil at Mach number 0.735, chord-based Reynolds number 1,000,000, and angle of attack 4°.

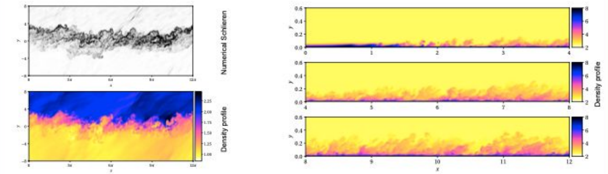

Direct numerical simulations of supercritical CO_2 planar shear layer at convective Mach number of 1 and transcritical CO_2 zero-pressure-gradient boundary layer with subcritical isothermal wall and supercritical freestream at Mach number 0.3.

Efficient parallel algorithm

- Solve linear systems arising from compact numerical schemes across distributed memory partitions
- Direct solver with deterministic operations
- Highly parallelizable on heterogeneous computing architectures
  - ✓ Considers both shared-memory and distributed-memory parallelisms
  - ✓ Low communication footprint avoiding repartitioning or transpose
- Scalable up to **24,576** GPUs in benchmark test on *Summit* supercomputer at the Oak Ridge Leadership Computing Facility (OLCF)

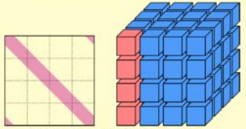

Schematic of a linear system formulated on distributed memory partitions with periodic "boundaries"

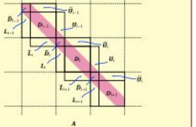

Logical partitions used in the linear solver

Block Gaussian elimination on distributed memory and formation of the reduced system

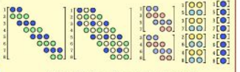

Schematics of parallel cyclic reduction (PCR)

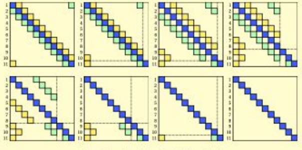

Schematics of parallel cyclic reduction (PCR)

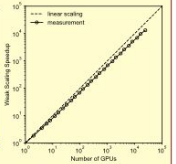

Weak scaling measurement

Ongoing developments: Mixed-precision operations

Real-gas models

- Equation-of-state for gases near critical temperature and pressure
- Fluids transport properties under high-pressure
- Consistent characteristic decomposition for Riemann solver

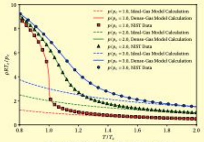

Dense-gas P-V-T relation calculated by Peng-Robinson equation-of-state model

Ongoing developments:
- Turbulent mixing under transcritical conditions
- Turbomachinery aerodynamics in supercritical fluids

ReachBot: A Small Robot for Mobility and Manipulation in Stochastic Environments

Marco Pavone

motion planner integrates stochastic limit surfaces,
meterized by pull angle and local rock geometry, to
mize the probability of gripper failure.
environment parameters in simulation are based
Martian-analog lava tube in the Mojave Desert.

Enabling technology:

- Extendable booms as controllable prismatic joints
- Lightweight, microspine grippers

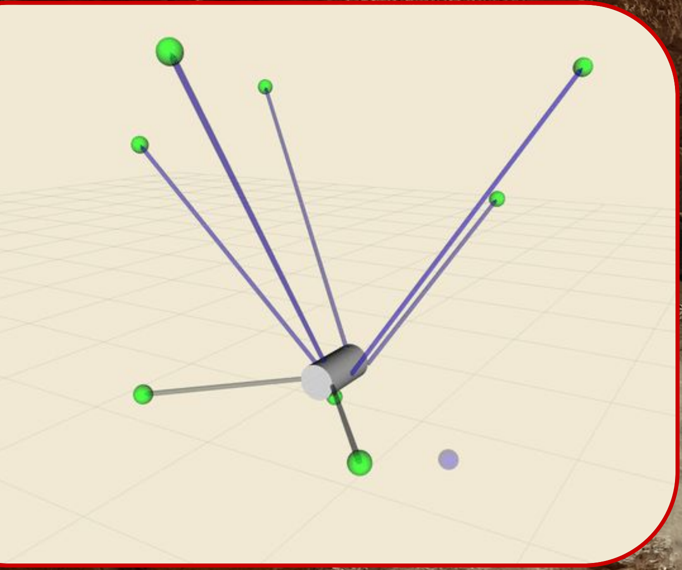

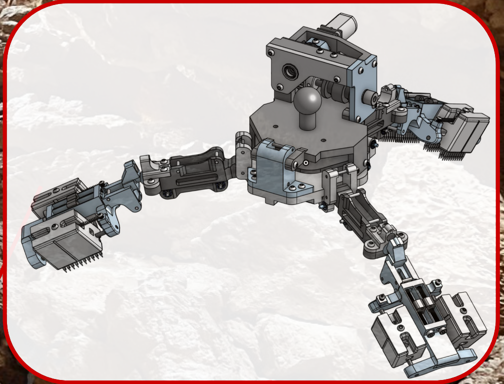

Stephanie Newdick
snewdick@stanford.edu

Dynamically Reprogrammable Stiffness in Gecko-Inspired Laminated Structures

Kai Jun Chen, Maria Sakovsky

Adaptive Structures: Applications

Robotic grippers

Glick et al. (2018)

Morphing Wing

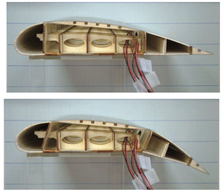

Kang et al. (2012)

Motivation

- **Reduce energy** use in structures with reprogrammable stiffness
- **Decouple stiffness modulation** from shape reconfiguration

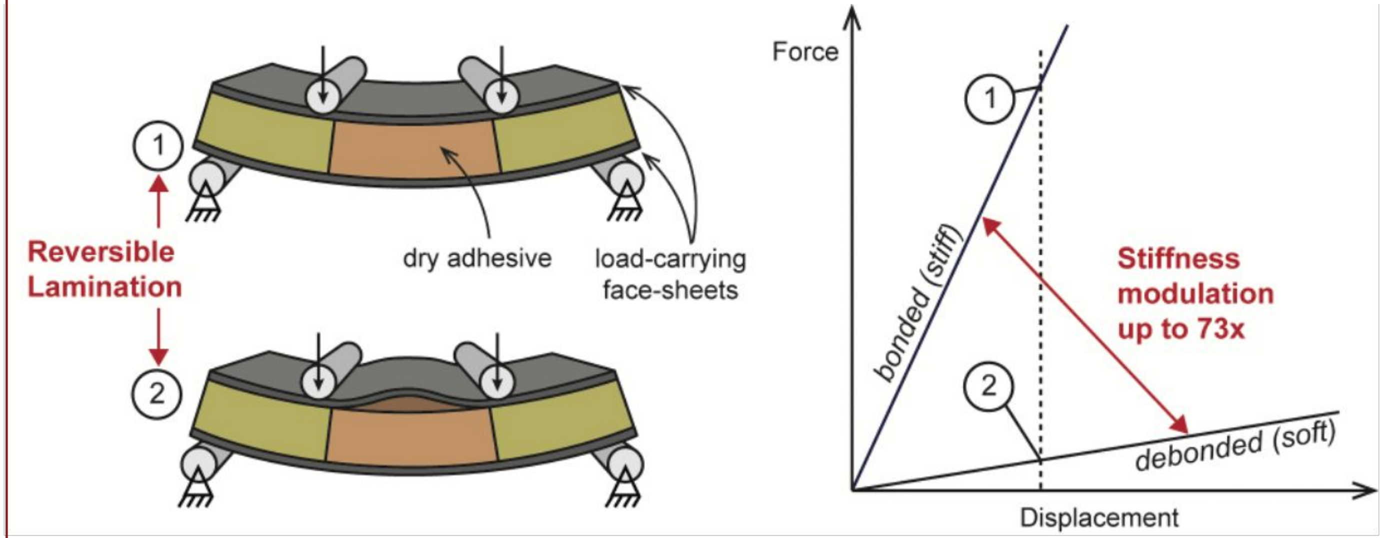

Stanford | Reconfigurable & Active Structures Lab

Guarantees on Robot System Performance Using Stochastic Simulation Rollouts

Joe Vincent*, Aaron Feldman*, Mac Schwager

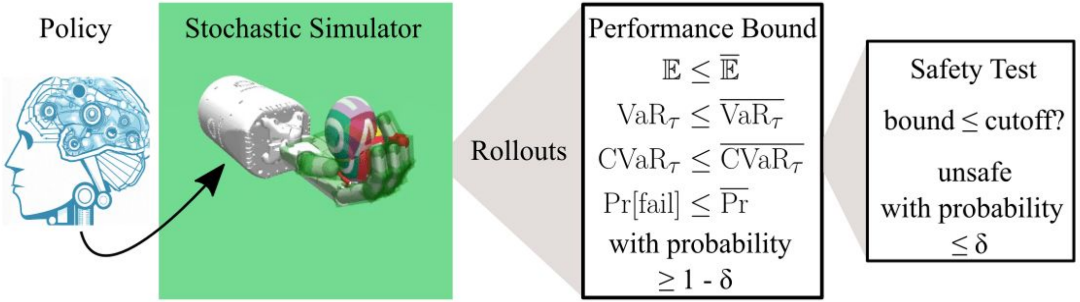

Policy

Stochastic Simulator

Rollouts

Performance Bound

$\mathbb{E} \leq \overline{\mathbb{E}}$

$\mathrm{VaR}_\tau \leq \overline{\mathrm{VaR}_\tau}$

$\mathrm{CVaR}_\tau \leq \overline{\mathrm{CVaR}_\tau}$

$\Pr[\mathrm{fail}] \leq \overline{\Pr}$

with probability $\geq 1 - \delta$

Safety Test

bound $\leq$ cutoff?

unsafe with probability $\leq \delta$

20-DOF Shadow Hand Example

- Mass uncertainty
- Friction uncertainty

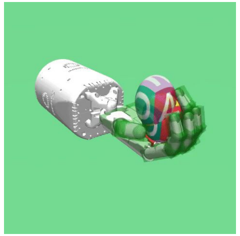

- Obtain bounds on expected value, VaR, CVaR, and failure probability given policy rollouts.
- Use bounds to test constraints on these quantities, achieving user-specified false acceptance rate.
- Select a least-risky policy among many options, using necessary bound corrections.

Bound Conservatism for Best Policy

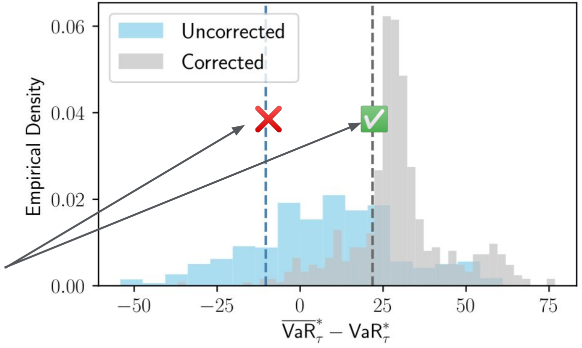

Dashed line should be above zero!

arXiv preprint

https://arxiv.org/abs/2309.10874

Effect of Growth Periods on Multi-physical Characterization of Mycelium Biocomposites

Victoria Porto, Kathryn Kornegay, Dr. Debbie Senesky

Scalability of Mycelium Biocomposites:

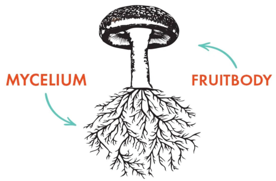

Fungi Components

Human Scale

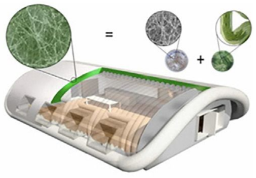

Habitat Scale

Mycelium Growth at different periods

30 days 60 days 120 days

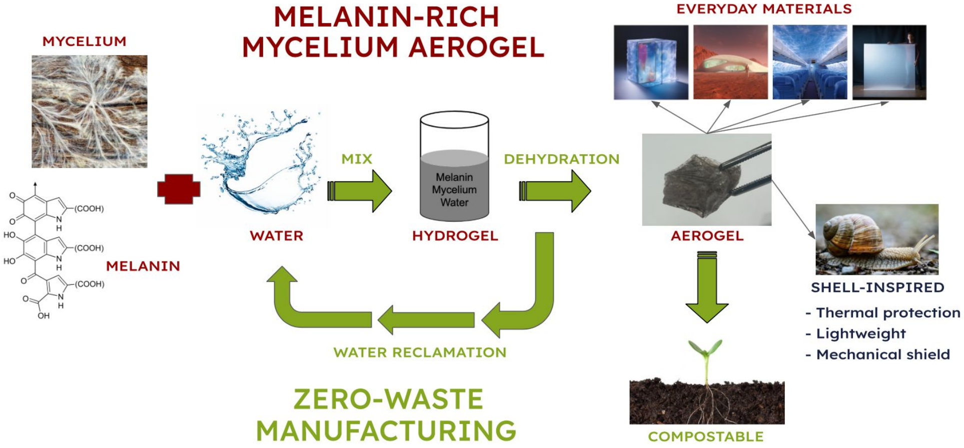

MELANIN-RICH MYCELIUM AEROGEL

MYCELIUM

MELANIN

WATER

MIX

HYDROGEL

Melanin
Mycelium
Water

DEHYDRATION

WATER RECLAMATION

ZERO-WASTE MANUFACTURING

EVERYDAY MATERIALS

AEROGEL

COMPOSTABLE

SHELL-INSPIRED
- Thermal protection
- Lightweight
- Mechanical shield

Frank Lai

Global Navigation Satellite System (GNSS)